

Orbital-Controlled Superconductivity in f -Electron Systems

Katsunori Kubo and Takashi Hotta

Advanced Science Research Center, Japan Atomic Energy Agency, Tokai, Ibaraki 319-1195, Japan

(Dated: February 25, 2019)

We propose a concept of superconductivity controlled by orbital degree of freedom by taking $CeMIn_5$ ($M=Co, Rh, \text{ and } Ir$) as typical examples. A microscopic multiorbital model for $CeMIn_5$ is analyzed by a fluctuation exchange approximation. Even though the Fermi-surface structure is unchanged, the ground state is found to change significantly among paramagnetic, antiferromagnetic, and d -wave superconducting phases, depending on the dominant orbital component in the band near the Fermi energy. We show that our picture naturally explains different low-temperature properties of $CeMIn_5$ by carefully analyzing the crystalline electric field states.

PACS numbers: 74.20.Mn, 71.70.Ch, 74.62.Bf, 65.40.De

Since the discovery of heavy-fermion superconductivity in $CeCu_2Si_2$ [1], it has been one of central issues in the research field of condensed matter physics to unveil unconventional superconductivity in strongly correlated electron systems. In particular, it is important to clarify a key parameter to control the appearance of superconductivity. Among heavy-fermion superconductors, $CeMIn_5$ ($M=Co, Rh, \text{ and } Ir$) have potential for systematic understanding of the mechanism and controlling parameter of superconductivity, since a variety of ordered phases has been found in the same crystal structure. At ambient pressure, a relatively high superconducting transition temperature $T_c=2.3$ K has been reported for $CeCoIn_5$ [2], while $T_c=0.4$ K for $CeIrIn_5$ [3]. On the other hand, $CeRhIn_5$ is an antiferromagnet with a Néel temperature $T_N=3.8$ K at ambient pressure, but it becomes superconducting with $T_c \simeq 2$ K under pressure $p \gtrsim 1.6$ GPa [4].

The observed power-law temperature dependence in specific heat [2, 5, 6], in thermal conductivity [5], and in spin-lattice relaxation rate [7] suggests the presence of line nodes in the superconducting gap function. In addition, four-fold magnetic-field angular-dependence in thermal conductivity [8] and in specific heat [9] clearly indicates d -wave superconductivity for $CeCoIn_5$. Existence of antiferromagnetism in $CeRhIn_5$ at ambient pressure is also consistent with d -wave superconductivity induced by antiferromagnetic fluctuations.

Concerning the controlling parameter of the superconductivity, one may first consider carrier density, as in the case of high- T_c cuprates. In addition, the Fermi-surface topology also plays a crucial role for the occurrence of superconductivity and the determination of symmetry of the gap function. However, the carrier density is essentially the same among $CeMIn_5$, since f -electron number per Ce ion is not changed by M . Furthermore, the Fermi surfaces observed by de Haas-van Alphen experiments and band-structure calculations are similar to each other among these compounds [10, 11]. Thus, neither the carrier density nor Fermi-surface topology is a main controlling parameter of superconductivity and antiferromagnetism in $CeMIn_5$.

Here we point out another important ingredient, crystalline electric field (CEF) effect, in $CeMIn_5$. Immediately after the discovery of $CeMIn_5$, Takimoto *et al.* have stressed the importance of the CEF effect to control the superconductivity [12], but only the level splitting was taken into account. We should note that a CEF potential changes not only the level splitting, but also the CEF ground-state wavefunction. In fact, recent inelastic neutron scattering experiments have revealed that the level splittings are almost the same among $CeMIn_5$, while the CEF wavefunctions are quite different [13]. The importance of orbital states has been discussed for $Na_xCoO_2 \cdot yH_2O$ [14], but the effects of the change in the orbital states on superconductivity have not been studied systematically so far. It is conceptually important to clarify superconductivity controlled by orbital states.

In this Letter, we apply a fluctuation exchange (FLEX) approximation to an f -electron model constructed on a square lattice for $CeMIn_5$. This model includes all the states with the total angular momentum $j=5/2$, which are split into one Γ_6 and two Γ_7 doublets under a tetragonal CEF. Among them, the wavefunctions of Γ_7 states sensitively depend on the CEF potential. We change the wavefunctions fixing the level splittings, and determine both T_c and T_N within the FLEX approximation. Even though the Fermi-surface structure does not change, the ground state changes depending on the Γ_7 wavefunctions among paramagnetic, antiferromagnetic, and d -wave superconducting states. We show that the obtained phase diagram is relevant to $CeMIn_5$.

By using the f -electron basis under a cubic CEF for convenience, we consider a three-orbital model based on a j - j coupling scheme on a square lattice [15], given by

$$H = \sum_{\mathbf{r}, \mu, \tau, \tau', \sigma} t_{\tau\tau'}^\mu c_{\mathbf{r}\tau\sigma}^\dagger c_{\mathbf{r}+\mu\tau'\sigma} + U \sum_{\mathbf{r}\tau} n_{\mathbf{r}\tau\uparrow} n_{\mathbf{r}\tau\downarrow} + (U'/2) \sum_{\mathbf{r}, \tau \neq \tau'} n_{\mathbf{r}\tau} n_{\mathbf{r}\tau'} + H_{\text{CEF}}, \quad (1)$$

where $c_{\mathbf{r}\tau\sigma}$ is the annihilation operator of f electron at site \mathbf{r} with pseudospin σ and orbital τ , $n_{\mathbf{r}\tau\sigma} = c_{\mathbf{r}\tau\sigma}^\dagger c_{\mathbf{r}\tau\sigma}$,

and $n_{\mathbf{r}\tau} = \sum_{\sigma} n_{\mathbf{r}\tau\sigma}$. We note that σ ($=\uparrow$ and \downarrow) distinguishes two states in each Kramers doublet. On the other hand, τ is introduced to distinguish three kinds of Kramers doublets under a cubic CEF. Here α and β denote two Γ_8 , while γ indicates Γ_7 . We use $t_{\tau\tau'}^{\mu}$ for the hopping amplitude between the τ' state at site $\mathbf{r}+\boldsymbol{\mu}$ and the τ state at \mathbf{r} , where $\boldsymbol{\mu}$ is a vector connecting nearest-neighbor sites. We consider the hopping through $(ff\sigma)$ bonding, given by $t_{\alpha\alpha}^{(a,0)} = t_{\alpha\alpha}^{(0,a)} = -\sqrt{3}t_{\alpha\beta}^{(a,0)} = -\sqrt{3}t_{\beta\alpha}^{(a,0)} = \sqrt{3}t_{\alpha\beta}^{(0,a)} = \sqrt{3}t_{\beta\alpha}^{(0,a)} = 3t_{\beta\beta}^{(a,0)} = 3t_{\beta\beta}^{(0,a)}$ and zero for the other cases [15], where $t=9(ff\sigma)/28$ and a is the lattice constant. The coupling constants, U and U' , denote intra- and inter-orbital Coulomb interactions, respectively. Note that we ignore the Hund's rule coupling and pair-hopping interaction for simplicity [15]. Then, due to the symmetry requirement, we should set $U=U'$.

The tetragonal CEF term, H_{CEF} , is given by

$$H_{\text{CEF}} = \sum_{\mathbf{r}} (B_2^0 O_{2\mathbf{r}}^0 + B_4^0 O_{4\mathbf{r}}^0 + B_4^4 O_{4\mathbf{r}}^4), \quad (2)$$

where B_m^n is the CEF parameter and $O_{m\mathbf{r}}^n$ is the Stevens operator equivalent at site \mathbf{r} [16]. We can rewrite Eq. (2) with the basis of the cubic CEF eigenstates as $H_{\text{CEF}} = \sum_{\mathbf{r}, \sigma, \tau, \tau'} B_{\tau\tau'} c_{\mathbf{r}\tau\sigma}^\dagger c_{\mathbf{r}\tau'\sigma}$, where $B_{\tau\tau'}$ is given by an appropriate linear combination of B_m^n . From the diagonalization of H_{CEF} , we express the CEF parameters as $B_2^0 = [-4\Delta_{67} + \Delta_7(2\cos(2\theta) - \sqrt{5}\sin(2\theta))]/84$, $B_4^0 = [3\Delta_{67} + \Delta_7(2\cos(2\theta) - \sqrt{5}\sin(2\theta))]/1260$, and $B_4^4 = \sqrt{5}\Delta_7(\sqrt{5}\cos(2\theta) + 2\sin(2\theta))/360$, where Δ_{67} and Δ_7 determine CEF energy levels, while θ characterizes eigenstates under a CEF potential. Then, the CEF energy levels are $-\Delta_{67}/3 - \Delta_7/2$ for $\Gamma_7^{(1)}$ states, $(c_{\mathbf{r}\gamma\sigma}^\dagger \cos\theta + c_{\mathbf{r}\alpha\sigma}^\dagger \sin\theta)|0\rangle$, $-\Delta_{67}/3 + \Delta_7/2$ for $\Gamma_7^{(2)}$ states, $(-c_{\mathbf{r}\gamma\sigma}^\dagger \sin\theta + c_{\mathbf{r}\alpha\sigma}^\dagger \cos\theta)|0\rangle$, and $2\Delta_{67}/3$ for Γ_6 states, $c_{\mathbf{r}\beta\sigma}^\dagger|0\rangle$, where $|0\rangle$ denotes the vacuum.

Now we apply FLEX approximation, which has been extended for multi-orbital models [17]. Since σ is a conserved quantity in the present model, the Green's function does not depend on σ and is represented by a 3×3 matrix. In a matrix form, the Dyson-Gorkov equation is given by $G(k) = G^{(0)}(k) + G^{(0)}(k)\Sigma(k)G(k)$, where $G(k)$ is the Green's function and $G^{(0)}(k)$ is the non-interacting Green's function. Here, we have introduced the abbreviation $k = (\mathbf{k}, i\epsilon_n)$, where \mathbf{k} is momentum and $\epsilon_n = (2n+1)\pi T$ is the fermion Matsubara frequency with an integer n and a temperature T . The self-energy is given by $\Sigma_{\tau_1\tau_2}(k) = \frac{T}{N} \sum_{q\tau_1'\tau_2'} V_{\tau_1\tau_1';\tau_2\tau_2'}(q) G_{\tau_1'\tau_2'}(k-q)$, where N is the number of lattice sites, $q = (\mathbf{q}, i\omega_m)$, and $\omega_m = 2m\pi T$ is the boson Matsubara frequency. The fluctuation exchange interaction is given by $V(q) = \frac{3}{2}[U^s\chi^s(q)U^s - U^s\chi^{(0)}(q)U^s/2 + U^s] + \frac{1}{2}[U^c\chi^c(q)U^c - U^c\chi^{(0)}(q)U^c/2 - U^c]$. The matrices U^s and U^c are given by $U_{\tau\tau';\tau\tau}^s = U_{\tau\tau';\tau\tau}^c = U$, $U_{\tau\tau';\tau\tau'}^s = -U_{\tau\tau';\tau\tau'}^c = U'$, and $U_{\tau\tau';\tau'\tau}^c = 2U'$, where $\tau \neq \tau'$, and the other matrix elements are zero. The spin and charge parts of the

susceptibility are given by $\chi^s(q) = \chi^{(0)}(q)[1 - U^s\chi^{(0)}(q)]^{-1}$ and $\chi^c(q) = \chi^{(0)}(q)[1 + U^c\chi^{(0)}(q)]^{-1}$, respectively, where $\chi_{\tau_1\tau_2;\tau_3\tau_4}^{(0)}(q) = -\frac{T}{N} \sum_k G_{\tau_1\tau_3}(k+q)G_{\tau_4\tau_2}(k)$.

In the FLEX approximation without the vertex corrections, the magnetic susceptibility is given by [18]

$$\chi_\nu(q) = \frac{1}{2} \sum_{\tau_1-\tau_4, \sigma_1-\sigma_4} \chi_{\tau_1\tau_2;\tau_3\tau_4}^s(q) J_{\tau_2\sigma_2;\tau_1\sigma_1}^\nu J_{\tau_3\sigma_3;\tau_4\sigma_4}^\nu \times \sigma_{\sigma_1\sigma_2}^\nu \sigma_{\sigma_4\sigma_3}^\nu, \quad (3)$$

where $\nu = x, y, \text{ or } z$, σ are the Pauli matrices, and $J_{\tau_2\sigma_2;\tau_1\sigma_1}^\nu$ is the matrix element of the operator of the dipole moment. In this paper, we renormalize J^ν so that the sum of squares of eigenvalues is unity, for convenience. The linearized equation for the anomalous self-energy, ϕ , is expressed as

$$\phi_{\tau_1\tau_2}^\xi(k) = -\frac{T}{N} \sum_{k'\tau_1'\tau_2'} K_{\tau_1\tau_2;\tau_1'\tau_2'}^\xi(k, k') \phi_{\tau_1'\tau_2'}^\xi(k'), \quad (4)$$

where ξ denotes the pseudospin singlet (S) or triplet (T) pairing state and the kernel is given by $K_{\tau_1\tau_2;\tau_1'\tau_2'}^\xi(k, k') = \sum_{\tau_3\tau_4} V_{\tau_1\tau_3;\tau_4\tau_2}^\xi(k - k') G_{\tau_3\tau_1'}(k') G_{\tau_4\tau_2'}(-k')$. The effective pairing interactions are given by $V^S(q) = \frac{3}{2}[U^s\chi^s(q)U^s + U^s/2] - \frac{1}{2}[U^c\chi^c(q)U^c - U^c/2]$ and $V^T(q) = -\frac{1}{2}[U^s\chi^s(q)U^s + U^s/2] - \frac{1}{2}[U^c\chi^c(q)U^c - U^c/2]$. The transition temperature of superconductivity is given by the temperature where Eq. (4) has a nontrivial solution.

In the following, we show results for a 32×32 lattice for $U=U'=4t$, $\Delta_{67}=1.5t$, and $\Delta_7=t$. In the calculation, we use 1024 Matsubara frequencies. The f -electron number per site is fixed as one, since we are considering Ce^{3+} ions. The present model with the CEF parameter θ is invariant for $\theta \rightarrow \theta + \pi$. In addition, when $U=U'$, the model is also invariant for $\theta \rightarrow -\theta$. Thus, it is enough to consider $0 \leq \theta \leq \pi/2$.

First let us discuss how the magnetic property changes depending on θ . Figures 1(a)–1(c) indicate the magnetic susceptibility $\chi_\nu(\mathbf{q}) = \chi_\nu(\mathbf{q}, i\omega_m=0)$ for $\theta=0, \pi/4$, and $\pi/2$, respectively. To understand such magnetic behavior, we show non-interacting band structures and Fermi-surface curves in Figs. 1(d)–1(i). Even if θ is changed, the dispersion around the Fermi level E_F is almost the same, leading to the similar Fermi-surface structure. However, the nearly flat band composed mainly of the γ orbital [19] is located near E_F for small θ , suggesting that electrons near E_F have nearly localized character. Thus, non-interacting susceptibility $\chi_\nu^{(0)}(\mathbf{q})$ for $\theta=0$ is almost flat in momentum space. With increasing θ , the localized character is weakened, and $\chi_\nu^{(0)}(\mathbf{q})$ shows structure in \mathbf{q} space. The magnitude of $\chi_\nu^{(0)}(\mathbf{q})$ becomes larger for smaller θ , since $\chi_\nu^{(0)} \sim \rho_0$ at enough low T , where ρ_0 is the density of states at E_F and it becomes large when localized nature is strong. Now we consider the effect of on-site Coulomb interactions, which suppress \mathbf{q} -independent part of $\chi_\nu^{(0)}(\mathbf{q})$.

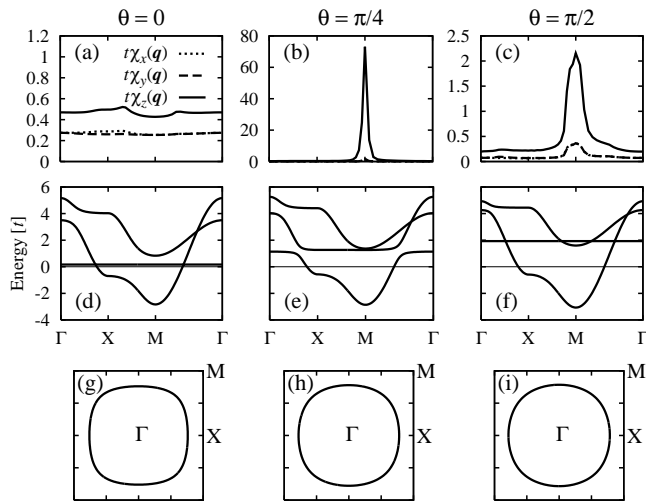


FIG. 1: (a)–(c) Magnetic susceptibility at $U=U'=4t$ and $T=0.02t$, for $\theta=0, \pi/4$, and $\pi/2$, respectively. (d)–(e) Energy band structures at $U=U'=0$ for $\theta=0, \pi/4$, and $\pi/2$, respectively. The Fermi energy is set as zero (thin lines). (g)–(i) Fermi-surface curves at $U=U'=0$ for $\theta=0, \pi/4$, and $\pi/2$, respectively. Parameters are set as $\Delta_{67}=1.5t$ and $\Delta_7=t$.

Thus, $\chi_\nu(\mathbf{q})$ for small θ is totally suppressed. Since the short-range Coulomb interactions enhance antiferromagnetic fluctuations, the structure in $\chi_\nu^{(0)}(\mathbf{q})$ grows to a peak at $\mathbf{q}=\mathbf{Q}\equiv(\pi/a, \pi/a)$ in $\chi_\nu(\mathbf{q})$. Such a peak becomes high and sharp, when the Coulomb interactions are effectively strong as for almost localized electrons for small θ . Thus, due to the combination of the band structure and the effect of the Coulomb interactions, $\chi_\nu(\mathbf{q})$ is large for a moderate value of $\theta\lesssim\pi/4$ with the peak at $\mathbf{q}=\mathbf{Q}$.

In Fig. 2, we show a T - θ phase diagram. In this paper, we define T_N as a temperature at which $\chi_z(\mathbf{Q})$ reaches $100/t$. Note that the susceptibility does not become as large as $100/t$ for the other components, χ_x and χ_y , or for \mathbf{q} other than \mathbf{Q} . The overall structure in Fig. 2 is consistent with the θ dependence of the magnetic property. Remark that a d -wave singlet superconducting state with B_{1g} symmetry appears at a region $0.29\pi\lesssim\theta$ next to the antiferromagnetic phase. In the other side of the antiferromagnetic phase, T_c is very low [20], even if the superconducting phase exists. This is consistent with the fact that the energy scale in the small- θ region becomes small due to strong localized nature.

Now we discuss possible relevance of our results to CeMIn_5 . For this purpose, it is necessary to estimate the value of θ for each material from the CEF eigenstates. Among the CEF parameters, the sign of B_4^4 is quite important, since the orbital state is drastically changed by the sign. Although inelastic neutron scattering is a powerful method to reveal the CEF energy levels, the sign of B_4^4 cannot be determined solely by the neutron scattering experiment. We should perform CEF analysis on a quantity sensitive to $\langle O_4^4 \rangle$, where $\langle \dots \rangle$ denotes the ex-

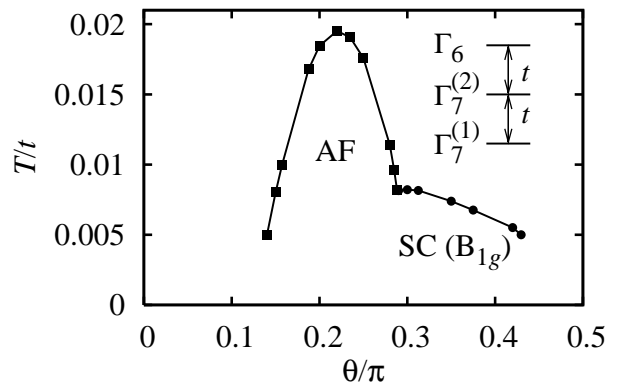


FIG. 2: Phase diagram for $U=U'=4t$, $\Delta_{67}=1.5t$, and $\Delta_7=t$. Solid squares denote antiferromagnetic (AF) transition temperature, while solid circles denote superconducting (SC) transition temperature with B_{1g} symmetry.

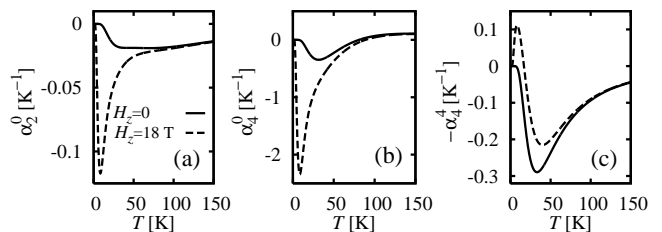


FIG. 3: Temperature dependence of (a) α_2^0 , (b) α_4^0 , and (c) $-\alpha_4^4$ for a single ion under the CEF potential deduced from neutron scattering experiments on CeRhIn_5 [13]. Solid curves denote the values without a magnetic field and dashed curves denote those in a magnetic field $H_z=18$ T along the c -axis.

pectation value in terms of H_{CEF} . Since the mode of charge distribution corresponding to finite $\langle O_4^4 \rangle$ couples to the lattice, thermal expansion is a good quantity to determine the sign of B_4^4 . Measurements of thermal expansion have been carried out for CeMIn_5 , but the analysis focused only on the second-order term $\langle O_2^0 \rangle$ [21, 22]. It is necessary to include fourth-order terms to analyze the thermal expansion, as for cubic systems [23].

Figures 3(a)–3(c) show the temperature dependence of $\alpha_2^0 \equiv d\langle O_2^0 \rangle/dT$, $\alpha_4^0 \equiv d\langle O_4^0 \rangle/dT$, and $\alpha_4^4 \equiv d\langle O_4^4 \rangle/dT$, respectively, for the CEF parameters deduced from the neutron scattering experiment for CeRhIn_5 [13], assuming $B_4^4 > 0$. For $B_4^4 < 0$, α_4^4 changes its sign, while α_2^0 and α_4^0 do not. Although we do not show the calculated results for CeCoIn_5 and CeIrIn_5 , it has been found that overall features are similar to each other among CeMIn_5 . Figures 3(a)–3(c) show that the magnetic-field effect on α_2^0 and α_4^0 is strong, while weak for α_4^4 . From the experimental results [22], the magnetic-field effect on the thermal expansion coefficient α_c along the c -axis for CeRhIn_5 is not so significant as found in Figs. 3(a) and 3(b). Rather it looks similar to Fig. 3(c). Moreover, the minimum with a negative value in $-\alpha_4^4$ shifts toward higher temperatures under a magnetic field, as is experimen-

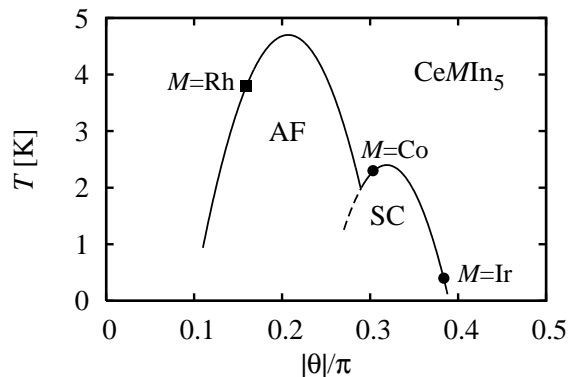


FIG. 4: Schematic phase diagram for $CeMIn_5$. Solid square and circles denote T_N and T_c , respectively. Curves are guides for eyes. See the main text for the values of θ .

tally observed in α_c of $CeRhIn_5$. Thus, we highly expect that α_c in $CeMIn_5$ is mainly determined by α_4^4 . For $CeCoIn_5$ and $CeIrIn_5$, α_c is always positive at temperatures reported [21], in sharp contrast to $CeRhIn_5$. These observations indicate that the signs of B_4^4 for $CeCoIn_5$ and $CeIrIn_5$ are the same, while they should be different from that for $CeRhIn_5$.

For further quantitative analysis, it is necessary to have more precise knowledge on elastic constants and/or magnetoelastic coupling, but it is out of the scope of this paper. Rather, we phenomenologically assume $B_4^4 > 0$ for $CeRhIn_5$. Then, B_4^4 is negative for $CeCoIn_5$ and $CeIrIn_5$. By using the CEF parameters deduced from the neutron scattering experiments [13], we obtain $\theta = 0.16\pi$ for $CeRhIn_5$, $\theta = -0.30\pi$ for $CeCoIn_5$, and $\theta = -0.38\pi$ for $CeIrIn_5$. In Fig. 4, we show a schematic phase diagram using these values of θ and experimental results for T_c and T_N . This is consistent with the theoretically determined phase diagram Fig. 2. In addition, $CeRhIn_5$ locates in a small- θ region, meaning that f electrons in $CeRhIn_5$ have relatively localized nature, as is suggested from de Haas-van Alphen experiments [11]. Thus, we conclude that the characteristics of $CeMIn_5$ can be captured by our model and the main controlling parameter of the antiferromagnetism and superconductivity for $CeMIn_5$ is θ which describes the CEF wavefunctions. To confirm our picture, it is interesting to perform experiments to determine CEF parameters for $CeMIn_5$ under pressure.

In summary, we have studied the f -electron model including all the states with $j=5/2$ within the FLEX approximation. We have found three kinds of ground states, i.e., paramagnetic, antiferromagnetic, and d -wave superconducting states, by changing the CEF wavefunctions characterized by a parameter θ , even if we fix the level splitting. Such phase change originating from the difference in the character of f -electron orbitals explains well the difference in $CeMIn_5$. This finding shows that, in general, orbital character can be a controlling param-

eter of superconductivity, in addition to the Fermi surface topology and carrier density. The orbital-controlled superconductivity would be realized also in other f -electron materials with active orbital degrees of freedom, and the present study will provide an important step toward investigations of such exotic superconductivity.

We are grateful to T. Takeuchi for sending us unpublished data of $CeCoIn_5$. We also thank T. Takimoto for useful discussions on FLEX calculation. K. K. is supported by the REIMEI Research Resources of Japan Atomic Energy Agency. T. H. is supported by the Ministry of Education, Culture, Sports, Science, and Technology of Japan.

-
- [1] F. Steglich *et al.*, Phys. Rev. Lett. **43**, 1892 (1979).
 - [2] C. Petrovic *et al.*, J. Phys.: Condens. Matter **13**, L337 (2001).
 - [3] C. Petrovic *et al.*, Europhys. Lett. **53**, 354 (2001).
 - [4] H. Hegger *et al.*, Phys. Rev. Lett. **84**, 4986 (2000).
 - [5] R. Movshovich *et al.*, Phys. Rev. Lett. **86**, 5152 (2001).
 - [6] R. A. Fisher *et al.*, Phys. Rev. B **65**, 224509 (2002).
 - [7] Y. Kohori *et al.*, Eur. Phys. J. B **18**, 601 (2000); G.-q. Zheng *et al.*, Phys. Rev. Lett. **86**, 4664 (2001); Y. Kohori *et al.*, Phys. Rev. B **64**, 134526 (2001); T. Mito *et al.*, Phys. Rev. B. **63**, 220507(R) (2001).
 - [8] K. Izawa *et al.*, Phys. Rev. Lett. **87**, 057002 (2001).
 - [9] H. Aoki *et al.*, J. Phys.: Condens. Matter **16**, L13 (2004).
 - [10] A. L. Cornelius *et al.*, Phys. Rev. B **62**, 14181 (2000); Y. Haga *et al.*, Phys. Rev. B **63**, 060503(R) (2001); D. Hall *et al.*, Phys. Rev. B **64**, 064506 (2001); R. Settai *et al.*, J. Phys.: Condens. Matter **13**, L627 (2001); T. Maehira *et al.*, J. Phys. Soc. Jpn. **72**, 854 (2003).
 - [11] H. Shishido *et al.*, J. Phys. Soc. Jpn. **71**, 162 (2002).
 - [12] T. Takimoto *et al.*, J. Phys.: Condens. Matter **14**, L369 (2002).
 - [13] A. D. Christianson *et al.*, Phys. Rev. B **70**, 134505 (2004).
 - [14] Y. Yanase, M. Mochizuki, and M. Ogata, J. Phys. Soc. Jpn. **74**, 430 (2005).
 - [15] T. Hotta and K. Ueda, Phys. Rev. B **67**, 104518 (2003).
 - [16] M. T. Hutchings, Solid State Phys. **16**, 227 (1964).
 - [17] T. Takimoto, T. Hotta, and K. Ueda, Phys. Rev. B **69**, 104504 (2004); M. Mochizuki, Y. Yanase, and M. Ogata, Phys. Rev. Lett. **94**, 147005 (2005); J. Phys. Soc. Jpn. **74**, 1670 (2005); K. Yada and H. Kontani, *ibid.* **74**, 2161 (2005).
 - [18] K. Kubo and T. Hotta, cond-mat/0512647.
 - [19] The hopping integrals including the γ orbital are zero in the present model. They are considered to be small in the square-lattice structure in general.
 - [20] For instance, we estimate $T_c \lesssim 0.00035t$ at $\theta = 0.139\pi$ by extrapolating the eigenvalues of the Kernel K in Eq. (4).
 - [21] T. Takeuchi *et al.*, J. Phys. Soc. Jpn. **70**, 877 (2001); T. Takeuchi *et al.*, J. Phys.: Condens. Matter **14**, L261 (2002); T. Takeuchi, private communication.
 - [22] V. F. Correa *et al.*, Phys. Rev. B **69**, 174424 (2004); V. F. Correa *et al.*, Phys. Rev. B **72**, 012407 (2005).
 - [23] P. Morin and S. J. Williamson, Phys. Rev. B **29**, 1425 (1984).